Biomedicine & Pharmacotherapy 170 (2024) 116025

Contents lists available at ScienceDirect

Biomedicine & Pharmacotherapy

journal homepage: www.elsevier.com/locate/biopha

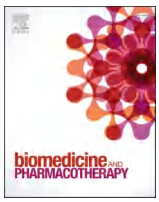

An organic state trace element solution for rheumatoid arthritis treatment by modulating macrophage phenotypic from M1 to M2

Shuangqing Wang [a,b], Jishan Yin [c], Yanhong Liu [a,b], Mingji Jin [a,b], Qiming Wang [a,b], Jianpeng Guo [d], Zhonggao Gao [a,b,*]

[a] State Key Laboratory of Bioactive Substance and Function of Natural Medicines, Institute of Materia Medica, Chinese Academy of Medical Sciences and Peking Union Medical College, Beijing 100050, China
[b] Beijing Key Laboratory of Drug Delivery Technology and Novel Formulations, Department of Pharmaceutics, Institute of Materia Medica, Chinese Academy of Medical Sciences and Peking Union Medical College, Beijing 100050, China
[c] Beijing JINSHAN Ecological Power element Manufactu Co., Ltd, Beijing 101300, China
[d] Key Laboratory of Natural Medicines of the Changbai Mountain, Ministry of Education, College of Pharmacy, Yanbian University, Yanji 133002, Jilin Province, China

ARTICLE INFO

Keywords:
Rheumatoid arthritis
Trace elements
Prophylactic
Macrophage phenotypic

ABSTRACT

Trace elements (TEs) are essential for the treatment of rheumatoid arthritis (RA). This study aimed to prepare a TEs solution enriched with various organic states to evaluate its preventive, therapeutic effects, and mechanism of action in RA and to provide a treatment method for RA treatment. The TEs in natural ore were extracted and added to 0.5% (W/V) L-alanyl-L-glutamine (LG) to obtain a TEs solution (LG-WLYS), which was examined for its concentration and quality. The antioxidant properties and effects of LG-WLYS on cell behavior were evaluated at the cellular level. The preventive and therapeutic effects and mechanism of action of LG-WLYS in rats with RA were explored. The LG-WLYS solution was clear, free from visible foreign matter, and had a pH of 5.33 and an osmolality of 305.67 mOsmol/kg. LG-WLYS inhibited cell migration and angiogenesis. LG-WLYS solution induced macrophages to change from M1-type to M2-type, increased the content of antioxidant enzymes (glutathione, superoxide dismutase, and IL-10), decreased the levels of nitric oxide, malondialdehyde, TNF-α, IL-1β, IL-6, COX-2, and iNOs, scavenging reactive oxygen species from the lesion site, inhibiting the apoptosis of chondrocytes, regulating inflammatory microenvironment, and decreasing inflammation response to exert the therapeutic effect for RA. In conclusion, LG-WLYS has outstanding therapeutic and preventive effects against RA and has enormous potential for further development.

1. Introduction

Rheumatoid arthritis (RA) is an autoimmune inflammatory disease characterized by synovial membrane hyperplasia, which leads to degeneration of articular cartilage and bone and damage to tendons and ligaments [1]. Clinical manifestations of RA include inflammation, swelling, pain, fatigue, and stiffness, which can lead to joint disability and deformity in severe cases, thereby affecting human health [2]. Therefore, effective treatment of RA is a critical task in medical research.

However, the exact pathogenesis of RA is still unclear. For many years, it has been believed that the pathophysiology of inflammatory diseases such as RA involves oxidative stress, an imbalance between the production of free radicals and the body's defensive antioxidant system [3]. Therefore, inflammation is considered a significant contributor to the pathogenesis of RA [4]. Aggravation of inflammation causes the accumulation of reactive oxygen species (ROS) and nitric oxide (NO), thus promoting the continuous occurrence of oxidative stress. Oxidative stress can lead to the abnormal conduction and proliferation of T lymphocytes, which can lead to disease flare-ups [5]. Treatment of RA aims to decrease joint inflammation and pain, increase joint function, and inhibit joint damage and deformities. Treatment of RA involves pharmaceuticals (non-steroidal anti-inflammatory drugs, disease-modifying antirheumatic drugs, and new biological agents), weight-bearing exercise, medical support, and rest. Glucocorticoids can lead to serious side effects, including bone loss and hyperglycemia. Frequent use of corticoids and glucocorticoids to block inflammatory cytokines can cause systemic immune suppression, leading to a high risk of infection and malignant tumors. In addition, not all patients respond to antibody

* Correspondence to: 1 Xian Nong Tan Street, Beijing, China.
E-mail address: zggao@imm.ac.cn (Z. Gao).

https://doi.org/10.1016/j.biopha.2023.116025
Received 22 August 2023; Received in revised form 2 December 2023; Accepted 14 December 2023
Available online 18 December 2023

therapy, and its benefits of using antibody therapy are transient [6]. Therefore, it is crucial to identify effective therapeutic measures to prevent in the occurrence and progression of RA.

Clinical studies have demonstrated that antioxidants significantly improve disease activity [7]. Metallic elements have considerable antioxidant properties [8]. The role of trace elements (TEs) in arthritis has received considerable attention because inflammatory responses are closely associated with TEs [8,9]. Impaired metabolism of TEs has been reported to play a role in the pathogenesis and progression of arthritis [10]. A case-control study found that blood cadmium, lead, urinary cadmium, antimony, tungsten, and uranium levels were positively associated with RA risk [11]. Serum zinc levels are low in patients with RA and negatively correlated with the levels of pro-inflammatory markers [12]. Intake of certain antioxidant micronutrients, particularly supplemental zinc, may be protective against the development of rheumatoid arthritis [13]. Epidemiological evidence suggests that higher cadmium concentrations in patients with RA may promote RA progression[14]. Low cadmium doses may protect against joint inflammation by controlling it and preventing cartilage destruction [15]. Selenium levels were significantly lower in patients with RA than in normal controls [16]. Plasma selenium levels are significantly reduced during mild to moderate and severe inflammation[17]. Most previous studies have assessed the association between single-element exposure and the risk of arthritis. Nevertheless, the human body is a complex living organism, and a single element does not reflect real-life situations.

However, the relationship between the pharmacological effects of multiple TEs and diseases is often overlooked. Supplementation with multiple TEs can more comprehensively meet the nutritional requirements of body, enhance the absorption and utilization rates of TEs, prevent and alleviate the symptoms of nutritional deficiencies caused by a single TE, and synergistically optimize the overall dietary effect. Currently, research on the pharmacological mechanism is lacking. This is especially true for diseases with unclear pathogenesis, for which existing drug treatments, such as RA, are ineffective.

Based on this, we developed a solution containing a multitude of TEs (LG-WLYS) to evalute their preventive and therapeutic effects on rats with RA and their antioxidant mechanisms to provide a new idea for clinical treatment. First, we prepared multiple TEs solutions containing 0.5% (w/v) L-alanyl-L-glutamine (LG). At the cellular level, we found that LG-WLYS decreased TNF-α, IL-1β, and IL-6 levels, increased IL-10 levels, inhibited cell migration and angiogenesis, accelerated the transformation of macrophages from M1 to M2. We evaluated the therapeutic effects and mechanisms of action of LG-WLYS in rats with RA. Finally, we explored the prophylactic effects of LG-WLYS in rats with RA and demonstrated that LG-WLYS prevented inflammatory diseases, reduced the cost of treatment, and alleviated patient pain.

2. Material and methods

2.1. Materials

Trace element (WLYS) solution was provided from Beijing Jingshan Ecology company (Beijing, China). L-Alanyl-L-Glutamine (99%) was purchased from Henan Yiduoyuan Biotechnology Co., Ltd. (Henan, China). Immunization Grade Bovine Type II Collagen (20022) and Incomplete Freund's Adjuvant (7002) were purchased from Chondrex (Washington State, USA). Cell Counting Kit-8 (C0038), Calcein AM Cell Viability Assay Kit (C2013M), Trizol (R0016), 4% Paraformaldehyde Fix Solution (P0099), Immunostaining Permeabilization Buffer with Triton X-100 (P0096), and QuickBlock™ Blocking Buffer for Immunol Staining (P0260) were obtained from Shanghai Beyotime Biotech. Inc. (Shanghai, China). Fetal bovine serum (26010074) was purchased from GIBCO LLC. (Grand Island, NY, USA). Reactive Oxygen Species Assay Kit (CA1410), Crystal violet (C8470, 1 mg/mL in water, AR), Penicillin-Streptomycin Liquid (P1400), DAPI solution (C0065, ≥ 90%, ready-to-use), BCA Protein Assay Kit (PC0020), Hoechst 33342 Stain solution (C0031, 1 mg/mL), and Matrigel Basement Membrane Matrix (356234) were purchased from Beijing Solarbio Science & Technology Co., Ltd (Beijing, China). RIPA Lysis Buffer (R917927) were obtained from Shanghai Macklin Biochemical Co., Ltd (Shanghai, China).

RAW264.7 and HUVECs were obtained from the Cell Culture Center of Institute of Basic Medical Sciences in Chinese Academy of Medical Sciences (CAMS, Beijing, China). and passages 7–20 were used. RAW264.7 and HUVECs were cultured in 75 cm^2 T-flasks in Dulbecco's Modified Eagle Medium supplemented with 10% (v/v) fetal bovine serum, and 1% (v/v) of a penicillin–streptomycin antibiotic blend in incubator (37 °C, 5% CO_2).

Male wistar rats (SPF, 6-week-old, 160–180 g) were obtained from Vital River Laboratory Animal Technology Co., Ltd. (Beijing, China). The animals were fed gamma-irradiated commercial rodent feed, and the facility used autoclaved water. The animals were given access to feed and water ad libitum. The environmental conditions were controlled with a temperature of 22 ± 2 °C, a relative humidity less than 70%, and a 12: 12-h light: dark cycle. All cages were assembled with bedding and furniture before being autoclaved, the cages were changed every 5 d and/or whenever necessary as determined by research personnel or the animal care team. All animal experiments were approved by the Laboratory Animal Ethics Committee in the Institute of Materia Medica and Peking Union Medical College (No. 00003493).

2.2. Preparation of LG-WLYS solution

LG-WLYS solutions were prepared by extracting TEs from natural ores. Briefly, (1) Natural ore powders were used, which include zinc ore powder, mica powder, vermiculite powder, coal ore powder, lapis lazuli powder, and mackerel powder, all of which were placed in a mixing tank. (2) At a temperature of 120–150 ℃ and a pressure of 3–6 atmospheres, a certain amount of dissolving solution was added. All of the dissolving solution was passed into the reaction tank, stirred at 50g for 4 h, and boiled at high temperature for 4 h to dissolve many metal ions in the dissolving solution. The dissolving solution was 3% dilute hydrochloric acid: 10% dilute sulfuric acid: 15% oxalic acid = 3:5:2 (v/v/v). (3) After the liquid is filtered by a lot of activated carbon, it flows into the alternating strong magnetic field, and driven by the alternating strong magnetic field. It is opened to the ultrasonic field for shearing and mixing. The time of action was 4 h and the strength of the magnetic field was $1 \times 10^{3-4}$ gauss. Then it was aged, filtered, and purified. (4) 0.9% sodium chloride was used as a diluent and passed into the above solution. (5) The solution was sterilized for 10 min using ozone at a concentration of 5 ppm, followed by UV irradiation for 3 h, and then filtered through a 0.45 μm microporous filter membrane to obtain WLYS solution. LG was added to the WLYS solution to obtain 0.5% (W/V) LG-WLYS solution.

2.3. Quality testing of LG-WLYS

The transparency, pH, and osmolality of the LG-WLYS solution were evaluated. The concentration of major TEs in the LG-WLYS solution was detected by Agilent 7500 ICP-MS (PlasmaQuant MS, Germany).

2.4. Cytotoxicity

RAW264.7 is the most commonly used in vitro research model for screening anti-inflammatory actives and studying inflammatory diseases.

2.4.1. CCK 8

To evaluate the effects of LG-WLYS on cell viability, CCK 8 assay was performed with RAW264.7 and HUVECs. RAW264.7 and HUVECs with 5×10^3 cells/well were seeded in 96-well plates and incubated at 37 ℃, respectively. After 12 h, the fresh medium containing LG-WLYS were

gently placed into each well to direct contact with the cells for 24 and 72 h. Then, the medium was discarded and replaced with serum-free culture medium containing 10% CCK 8 solution. After 2 h of incubation, the OD value of each well was measured at a wavelength of 450 nm by a Synergy H1 Microplate Reader (BioTek, Dallas, TX, USA) (n = 6).

2.4.2. Live and dead cell staining

The biocompatibility was evaluated by Calcein-AM/PI staining. Briefly, RAW264.7 cells were seeded in 24-well plates and incubated. The cells were activated by LPS for 24 h as the Model group. After 24 h, the fresh medium containing WLYS, LG, and LG-WLYS were gently placed into each well for 24 and 72 h. The cells were stained with 300 μL Calcein-AM/propidium iodide and then further co-cultured at 37 °C for 30 min. Finally, cells were observed by a CLSM (Biotek, Winooski, VT, USA).

2.4.3. Apoptosis

Apoptosis of RAW264.7 cells was evaluated by Hoechst 33342 staining solution. RAW264.7 cells were seeded on 24-well plates with 2×10^4 cells/wells and incubated. The cells were activated by 1 μg/mL LPS for 24 h as the model group. The fresh medium containing different reagents were gently placed into each well for 72 h. Then, the nuclei were stained by Hoechst 33342 staining solution for 10 min. Finally, the nuclei were observed by a CLSM.

2.5. ROS staining

The cell-permeable DCFH-DA was applied to measure the ROS levels in RAW264.7 cells. Briefly, RAW264.7 were seeded separately in 12-well plates at a density of 1×10^5 cells/well. The cells were activated by 1 μg/mL LPS for 24 h. Cells were co-cultured with different preparations for 12 and 24 h. RAW264.7 cells were treated with 0.5 mL of 10 μmol/L DCFH-DA in the free-medium for 30 min. The fluorescent images were visualized by a CLSM.

2.6. Cell scratch

The anti-migration ability of LG-WLYS was evaluated by cell scratch assay. HUVECs cells were plated in 6-well plates at a density of 2×10^5 cells/well and cultured until they formed a monolayer. Subsequently, the cell monolayer was scraped using a 200 μL pipette and washed three times with PBS. The cells were incubated with different preparations, and cell images were captured with an inverted light microscope (Olympus, Hamburg, Germany) at specific times (0, 12, and 24 h). Scratch healing rate (%) = $(C_0 - C_t) / C_0 \times 100\%$.

In where, C_0 and C_t separately represent the scratch area before and after an intervention.

2.7. Vertical migration

HUVECs cells were seeded in the upper chamber of the transwell (costar 3422, 8.0 μm pore size) with a density of 1×10^5 cells/well. And 200 μL of free media containing different formulations were added. After 12 h, the non-migrated cells in the upper chamber were removed with a cotton swab. The cells on reverse side were fixed in 4% paraformaldehyde. The cells were stained with a crystal violet staining solution (200 μL) for 15 min. The cells were observed under a microscope and the characteristics of vertical migration were evaluated. The number of cells migrated to the lower insert was calculated by ImageJ (National Institutes of Health, Bethesda, MD, USA).

2.8. Tube formation assay

The effect of LG-WLYS solution at this concentration on angiogenesis was evaluated by tube formation assay. Frozen Matrigel was thawed on ice. Then, 50 μL of Matrigel was added to precooled 96-well plates, then placed at 37 °C for 1 h. HUVECs were seeded into well plates at a density of 2×10^5 cells/well. The cells were incubated with 100 μL different preparations. After 6 h, tube formation images were obtained by a microscope, and the total length and number of junctions were analyzed by ImageJ in five random fields.

2.9. Determination of cytokines

The levels of various cytokines were measured to assess the anti-inflammatory activity of the LG-WLYS. RAW264.7 were pre-treated with LPS for 24 h. Afterward, different preparations (LPS, WLYS, LG, LG-WLYS, and DMEM) were added for further incubation for 24 h. The supernatant was gently aspirated and collected. The levels of cell cytokines (TNF-α, IL-1β, IL-6, and IL-10) were determined with enzyme-linked immunosorbent assay (ELISA) kits (Enzyme-Link Biotech, Shanghai, China).

Total RNA was isolated from eWAT using the TRIzol reagent and the RNA was quantified using a Nano-300 Micro-Spectrophotometer (All-Sheng, Hangzhou, China). cDNA was synthesized from 1 μg of RNA with a reverse transcription system (Promega, Madison, WI, USA). RT-qPCR was performed by a protocol consisting of 40 cycles of 30 s at 95 °C, 10 s at 95 °C, and 30 s at 60 °C. Melting curve analysis was used to determine the purity of the PCR products. The used primers in this experiment are listed in Table S1 in the Supplementary Information.

2.10. Macrophage phenotype transition study

Polarization of RAW264.7 macrophages was characterized by immunofluorescence staining. RAW264.7 were seeded in 12-well plates at a density of 2×10^5 cells/well and cultured for 12 h. The cells were induced by LPS and then incubated with the different formulations for 24 h. RAW264.7 were permeabilized with Triton X-100 for 30 min. Next, they were blocked at 37 °C for 1 h. Next, cells were incubated with iNOs (1:400) and CD106 (1:500) overnight at 4 °C, followed by a fluorescent secondary antibodies incubation for 1 h at 25 °C. The nuclei were stained with DAPI for 10 min. The immunofluorescence images of the cells were taken by a CLSM.

2.11. In vivo animal experiments

2.11.1. Establishment of RA model

Rats were subcutaneously injected in the tail with bovine type II collagen (2 mg/mL) and incomplete Freunds adjuvant (2 mg/mL). About 200 μL of the emulsion was injected into rat tails as initial immunizations. After 7 d, rats were again immunized with 100 μL emulsion as a booster injection. The success of model establishment was evaluated by inflammatory scores of rat joints. After 21 d, the rats were randomly divided into the Model, WLYS, LG-WLYS, LG-$WLYS_{oral}$, and Positive (Methylethalin, oral, 0.5 mL, 1.8 mg/kg). The healthy rats served as the Control group. There were six rats in each group. A total of 36 rats were used. In WLYS and LG-WLYS group, 0.05 mL was injected through the joint cavity using a 1 mL syringe. The frequency of administration was once every 3 d, and the administration cycle was 30 d. The body weight, paw thickness, and arthritis score of rats were recorded every 3 d. The clinical arthritis score was the cumulative score of the 4 limbs (the maximum score for each rat was 16).

2.11.2. Toxicity and histopathological analysis

To evaluate the safety of each preparation, the serum of rats was collected after treatment, and the levels of aspartate aminotransferase (AST), alanine aminotransferase (ALT), blood urea nitrogen (BUN) and creatinine (CREA) were measured by using the standard kits (Nanjing jiancheng, Nanjing, China) according to the manufacturer's instructions [18].

After treatments, all the rats were euthanized by inhalation of an excess of isoflurane. The ankle joints and main organs (heart, liver,

spleen, lung, kidney, stomach, and brain) of some rats were collected and fixed in 4% paraformaldehyde[19]. The ankle joints were decalcified with 10% EDTA solution for 30 d at 25 ℃. Samples were embedded in paraffin and sliced into 5 μm thick sections. The sections of ankle joints and main organs were stained with H&E staining. And the sections of ankle joints were Masson staining, Safranin-O-staining, TRAP staining, TUNEL staining, ROS staining, immunohistochemistry (iNOs and CD163), Western blot (TNF-α and IL-6), and immunofluorescence staining (TNF-α, IL-1β, IL-6, and IL-10).

2.11.3. Organ index

After the end of treatment, the spleen and thymus of rats were collected. Adipose tissue was removed from surface and the tissue fluid was aspirated with filter paper. Organ index = Organ weight (mg) / Body weight (g).

2.11.4. X-ray

X-ray imaging was performed on the rat toes and ankle joints to assess bone destruction. The isolated bone tissues were fixed with 4% paraformaldehyde before X-ray was taken. The differences in inflammation between the groups were evaluated from bone erosion, joint space, and bone destruction.

2.11.5. Inflammatory factor assay

Synovial tissues were shredded (800g, 20 s with 10 s interval gap) and homogenized in 1 mL of pH 7.4 PBS. Inflammatory cytokines such as TNF-α, IL-1β, IL-6, IL-10, NO, GSH, MDA, and SOD were estimated using Elisa kit following the standard instructions.

For RT-qPCR detection (*Tnf-α, Il-1β, Il-6,* and *Il-10*), some synovial tissues were shredded and homogenized in 1 mL of TRIzol Regent (Vazyme, Nanjing, China). A total amount of 1 μg total RNA were reversely transcribed by the transcription kit (Vazyme, Nanjing, China) following the standard instructions with a LightCycler 96 Real-Time PCR System. SYRB Green RT-qPCR was performed using specific primers (Table S1). A qPCR system with GAPDH as internal reference was established. The results were evaluated with the comparative threshold cycle ($2 - \Delta\Delta Ct$) method.

The synovial tissues were homogenized (2500 rpm) thrice for 20 s with 10 s interval gap by placing the homogenizer tube on ice. The homogenization was followed by sonication and centrifuged at 5000 g for 10 min. The supernatants were retrieved and protein concentrations were measured with the BCA protein assay kit. The proteins were separated by sodium dodecyl sulfate–polyacrylamide gel electrophoresis gel and transferred to 0.22 μm pore size PVDF membrane. The membrane was incubated with specific primary antibodies at 4 ℃ overnight. Next day, the membranes were incubated with corresponding secondary antibodies at 25 ℃ for 1 h. Then protein blots were detected by chemiluminescene reagent in a dark environment. Protein bands densities were measured using Image J.

2.12. Prophylactic experiment

The effectiveness of the LG-WLYS intervention in inflammatory diseases was examined by setting up a prevention group. Healthy rats (n = 6) were given a 200-fold dilution of LG-WLYS ad libitum every day for 20 d. At the same time, a control group (n = 6) was set up, and the rats in the control group drank pure water every day. A total of 12 rats were used. Changes in body weight were recorded daily during the period. Primary immunization was performed on the 21st d. After that, it was replaced with LG-WLYS diluted 10 times. The second immunization was performed on the 28th d. The specific operation is the same as "2.11.1 Establishment of RA model". The body weights and morbidity of the rats were recorded afterwards. All rats were euthanized by inhalation of an excess of isoflurane at 51 d. Histopathologic analyses of the ankle joints of the rats were performed, such as H&E, Masson staining, Safranin-O-staining, and TRAP staining.

2.13. Statistical analysis

All data were presented as mean ± standard deviation and each experiments was performed at least three times. Statistical analysis was tested with the Prism 7.0 software (GraphPad Software) by Tukey's multiple comparison tests and one-way analysis of variance. The differences were considered significant, when p values $^{*} < 0.05$, $^{**} < 0.01$, and $^{***} < 0.001$.

3. Results

3.1. Quality testing of LG-WLYS

The LG-WLYS solution was clear, free from visible foreign matter, and had a pH of 5.33 and an osmolality of 305.67 mOsmol/kg. This solution complied with the Pharmacopoeia of the People's Republic of China (2020). After ICP-MS detection, the iron concentration was 38.40 mg/L, magnesium was 35.80 mg/L, aluminum was 29.20 mg/L, zinc was 12.12 mg/L, manganese was 3.08 mg/L, titanium was 2.08 mg/L, calcium was 1.71 mg/L, selenium was 0.42 mg/L, vanadium was 0.13 mg/L, nickel was 0.09 mg/L, cobalt was 0.08 mg/L, molybdenum was 0.03 mg/L, cobalt was 0.02 mg/L, and copper was 0.02 mg/L. There were also dozens of barium, copper, potassium, iodine, chromium, and other TEs.

3.2. Cytotoxicity

In this study, we investigated the viability of RAW264.7 and HUVECs cultured with different concentrations of LG-WLYS for 24 and 72 h, respectively. CCK 8 results showed that LG-WLYS did not notably inhibit cell viability in the concentration range examined (10–1000-fold dilution) and even promoted cell proliferation at high concentrations (Fig. 1 A and B). After LPS induction, some RAW264.7 were stained red (dead) (Fig. 1 C and D). After incubation with LG-WLYS, a large amount of RAW264.7 stained green (live), and the number of cells increased noteworthy, demonstrating the excellent biocompatibility of LG-WLYS. Nuclear disruption occurred in RAW264.7 after LPS induction (Fig. 1 E and F). The nuclear morphology remained intact after LG-WLYS treatment. These results demonstrated that LG-WLYS is biocompatible and promotes cell proliferation at appropriate concentrations. Subsequent cell experiments were performed using 10-fold diluted LG-WLYS.

3.3. ROS

After LPS induction, RAW264.7 produced a large amount of ROS (green fluorescence) (Fig. 2 A and B). After treatment with LG-WLYS, ROS levels was reduced ($P < 0.001$), and the effect was pronounced with increasing incubation time, showing a time dependence. These results revealed that LG-WLYS is a promising candidate for relieving oxidative stress during RA treatment.

3.4. Cell behavior

Microvessels are hallmark of RA. First, the horizontal migration of HUVECs was evaluated. VEGF acts as an effective proangiogenic factor [20]. LG-WLYS inhibited VEGF-induced cell migration (Fig. 2 C and F). Similar results were obtained in the Transwell assays (Fig. 2 D and G). In the tube formation assay, LG-WLYS inhibited angiogenesis ($P < 0.001$) (Fig. 2 E and H). These above results suggested that LG-WLYS can modulate endothelial cell behavior and inhibit angiogenesis in the inflammatory microenvironment.

3.5. Antioxidant mechanisms

Clinical evidence shows that the number of macrophages is significantly increased in RA patients with inflammatory tissue. Macrophages

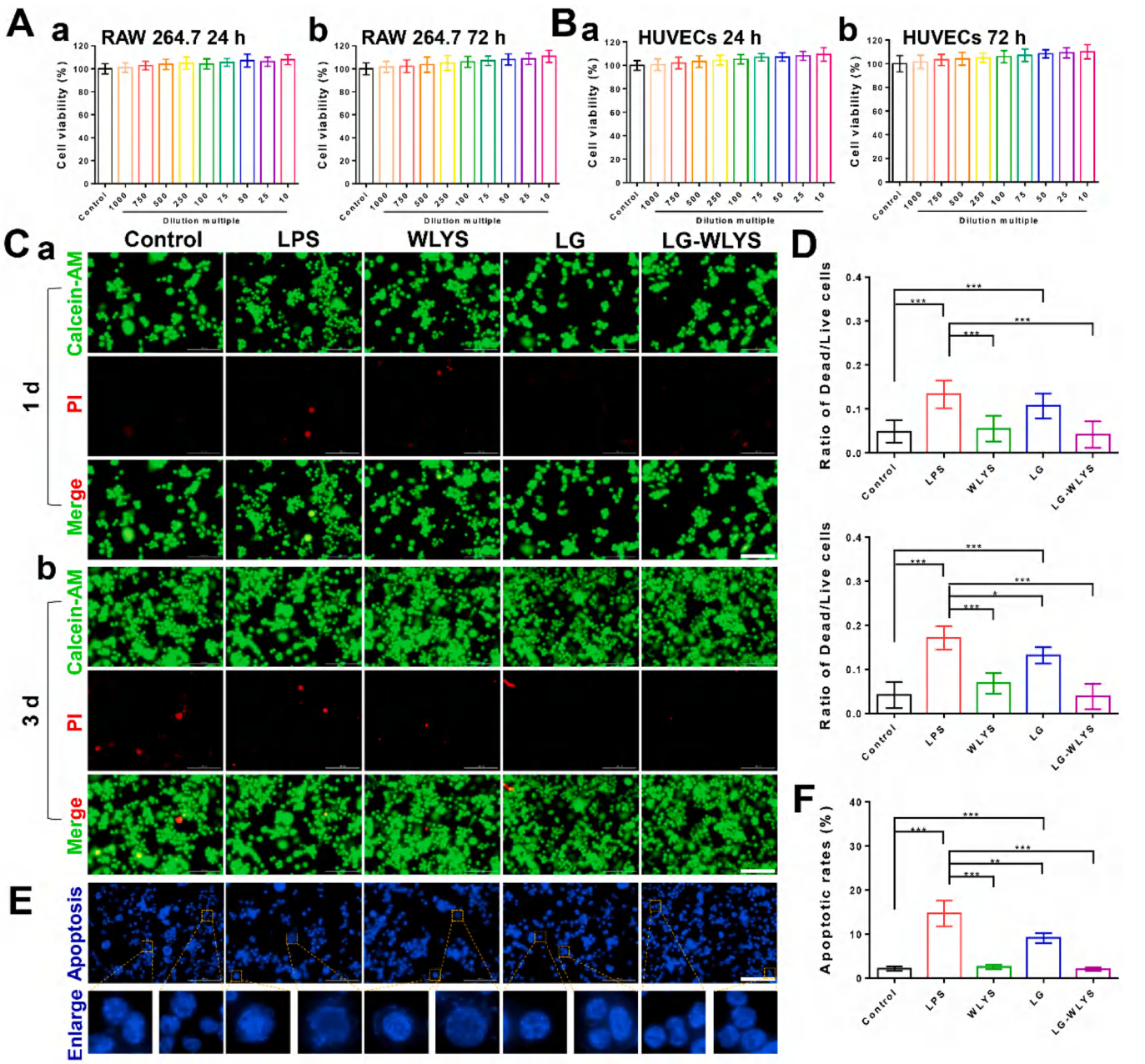

Fig. 1. Biocompatibility. (A) RAW264.7 viability with different concentrations at (a) 24 and (b) 72 h (n = 6, mean ± SD). (B) HUVECs cell viability with the different preparations at (a) 24 and (b) 72 h (n = 6, mean ± SD). (C) Live and dead staining of RAW264.7 after incubation with different concentrations for (a) 1 and (b) 3 d. Scale bar = 200 μm. (D) Ratio of Dead/Live RAW264.7 cells (n = 6, mean ± SD). (E) CLSM images of RAW264.7 with Hoechst staining after 24 h of incubation with different concentrations for 1 d. Scale bar = 200 μm. (F) Apoptotic rate (n = 3, mean ± SD). * $P < 0.05$, * * $P < 0.01$, * ** $P < 0.001$.

with different phenotypes play crucial roles in the inflammatory cascade. The M1 phenotype produces inflammatory cytokines that accelerate the oxidative processes and inhibit tissue repair. The M2 phenotype produces anti-inflammatory cytokines, reduces the release of inflammatory factors, and enhances tissue repair and antioxidant activity. An imbalance in M1/M2 balance leads to multiple inflammatory responses. The cells not only secret pro-inflammatory cytokines (TNF-α, IL-6, and IL-1β) but also accelerate the apoptosis of chondrocytes. TNF-α and IL-1β have synergistic actions, and their interaction mediates joint damage and inflammatory responses. IL-10 is an essential anti-inflammatory cytokine that effectively suppresses effector T cell responses. ELISA assays were applied to test TNF-α, IL-1β, IL-6, and IL-10 levels. LG-WLYS reduced TNF-α, IL-1β, and IL-6 and increased IL-10 ($P < 0.001$) (Fig. 3 A). This result was consistent with the results of RT-qPCR (Fig. 3 B).

Accelerated macrophage polarization from the M1 to the M2 phenotype contributes to the alleviation of inflammatory diseases. The addition of LPS induced the M1 phenotype (iNOs) of RAW264.7 macrophages. In contrast, the addition of LG-WLYS induced the M2 phenotype (CD163), indicating a change toward M2 macrophages (Fig. 3 C and D). Flow cytometry also revealed a change in macrophage phenotype (Fig. 3 E), which was consistent with the immunofluorescence results. This showed that LG-WLYS exerted anti-inflammatory effects by promoting macrophage transition from the M1 to the M2 phenotype.

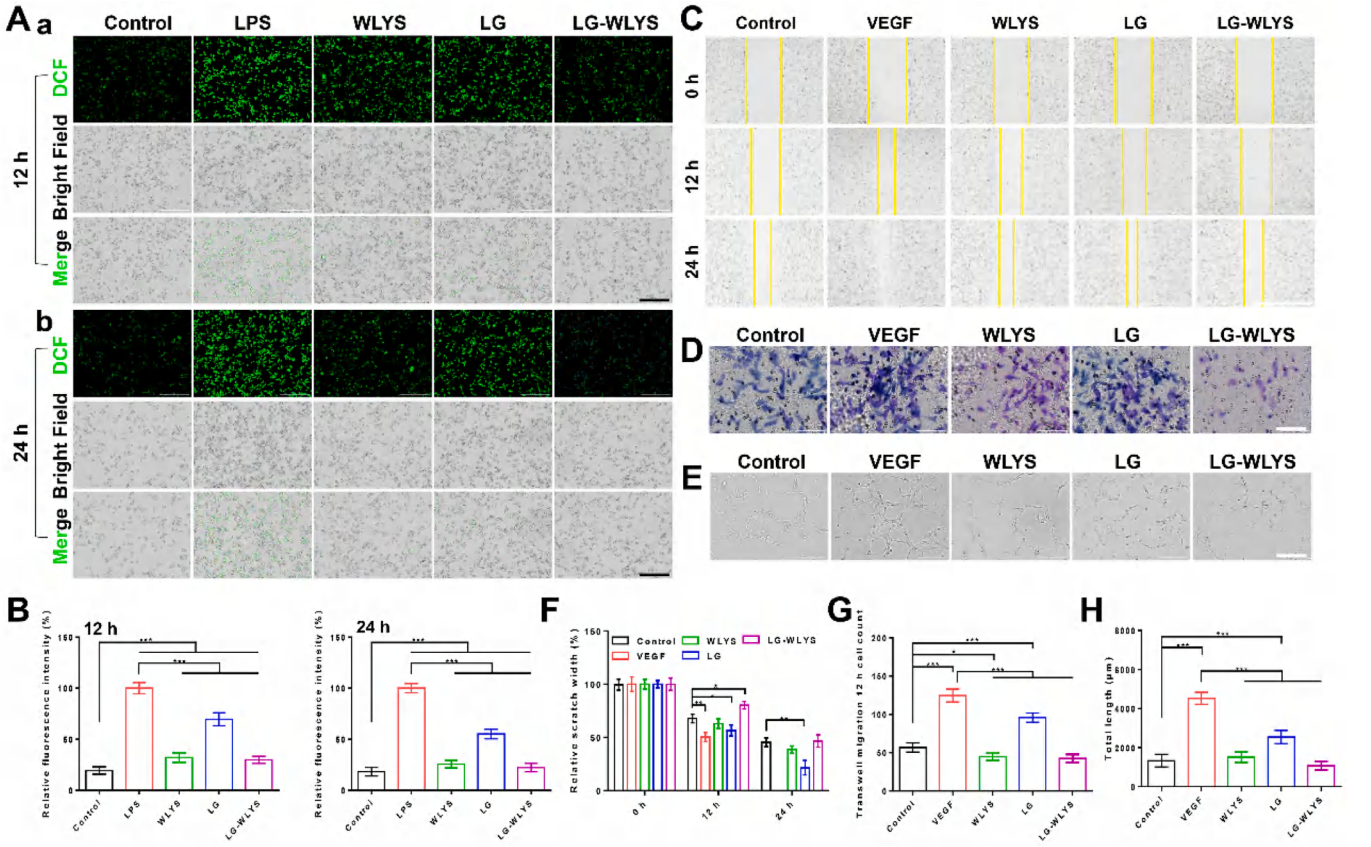

Fig. 2. Cell behavior studies. (A) ROS staining of RAW264.7 with different concentrations at (a) 12 and (b) 24 h. Scale bar = 200 μm. (B) Quantitative results of the fluorescence intensity of ROS staining (n = 6, mean ± SD). (C) Healing rates of cell scratch during 24 h. Scale bar = 1000 μm. (D) The ability of different concentrations to migrate vertically. Scale bar = 200 μm. (E) Tube formation capacity of HUVECs after incubation with different concentrations for 6 h. Scale bar = 200 μm. (F) Scratch healing rate (n = 3, mean ± SD). (G) Transwell migration 12 h HUVECs cells count (n = 6, mean ± SD). (H) Quantitative results of total length by HUVECs incubated in different preparations for 6 h (n = 6, mean ± SD). * $P < 0.05$, * * $P < 0.01$, * ** $P < 0.001$.

3.6. RA

The anti-arthritic effects of LG-WLYS in vivo and its mechanism of action as an active ingredient were evaluated in CIA rats. Methotrexate (MTX), the gold standard treatment for RA, was used as a positive group. Fig. 4 A shows flowchart of the animal experiment. The rats gradually lost weight (Fig. 4 C), and exhibited paw swelling (Fig. 4 B and D), tail nodes, and erythema after the onset of RA. The body weight of CIA rats increased slowly. After LG-WLYS was administered by intra-articular injection, weight gain was accelerated, paw thickness was reduced, and arthritis scores were reduced (Fig. 4 E). After 48 days, the rats recovered their body weight (Fig. 4 F), and the paw thickness of the LG-WLYS group did not differ from that of the control group (Fig. 4 G). The LG-WLYS group showed the lowest arthritis score (Fig. 4 H). These results demonstrated significant relief of RA symptoms after intra-articular injection LG-WLYS. The therapeutic effect in the LG-$WLYS_{oral}$ group was similar to that of the positive group. This indicated that the oral administration of LG-WLYS also slightly relieved RA symptoms.

The pathological state of RA is related to continual synovitis, and progressive cartilage and bone destruction [21]. The progression or recovery of the rats with RA following LG-WLYS administration was verified by evaluating the status of bone, cartilage, and synovium from days 48. Synovial hyperplasia and joint structure of RA rats were observed by H&E staining (Fig. 5 A), Masson staining, Safranin-O-staining, and TRAP staining. In the Model group, remarkable pathological changes were observed in the joints, including synovial tissue hyperplasia, vascular expansion, fibrosis, synovial tissue adhesion, joint soft tissue destruction, bone erosion, pannus formation, accompanied by many inflammatory cell infiltration and cell arrangement disorders. LG-WLYS enhanced the pathology and dramatically decreases the symptoms of synovial hyperplasia, inflammatory cell infiltration, and cartilage infiltration. The LG-WLYS group showed a normal morphology of massive new bone tissue. This reduced the absorption of bone tissue and effectively alleviating the erosion and destruction of bones and joints. LG-WLYS reduced the histopathological and Mankin scores ($P < 0.001$) (Fig. 5 B). These results indicated that LG-WLYS improved RA symptoms in CIA rats.

Compared with healthy rats, the ankle joints of the model rats showed apparent bone erosion and structural damage (Fig. 5 C). However, bone damage and erosion significantly reduced after treatment with LG-WLYS. Similarly, the quantitative analysis of the morphological parameters of the ankle trabecular bone measured by X-ray also proved the practical therapeutic effect of LG-WLYS (Fig. 5 D).

An imbalance between inflammatory and anti-inflammatory cytokines is the main factor that causes the initiation and progression of RA. We found that TNF-α, IL-1β, and IL-6 levels in the model group rats were increased ($P < 0.001$) (Fig. 6 A), reiterating that the abnormal expression of inflammatory indicators in the rats with RA was closely related to joint injury. Compared with the model group, TNF-α, IL-1β, and IL-6 were decreased ($P < 0.001$), and IL-10 was increased ($P < 0.001$) in the WLYS and LG-WLYS groups. Gene expression (Fig. 6 B) and immunofluorescence results (Fig. 6 C) of the inflammatory factors were consistent with the ELISA results. TNF-α and IL-6 levels measured by western blot also showed similar trends (Fig. 6 D). Meanwhile, these results were compatible with those of the cellular studies. These results suggested that LG-WLYS exerted anti-inflammatory effects in CIA rats.

Inflammatory and biochemical markers are essential for predicting the clinical response and monitoring joint damage. Malondialdehyde

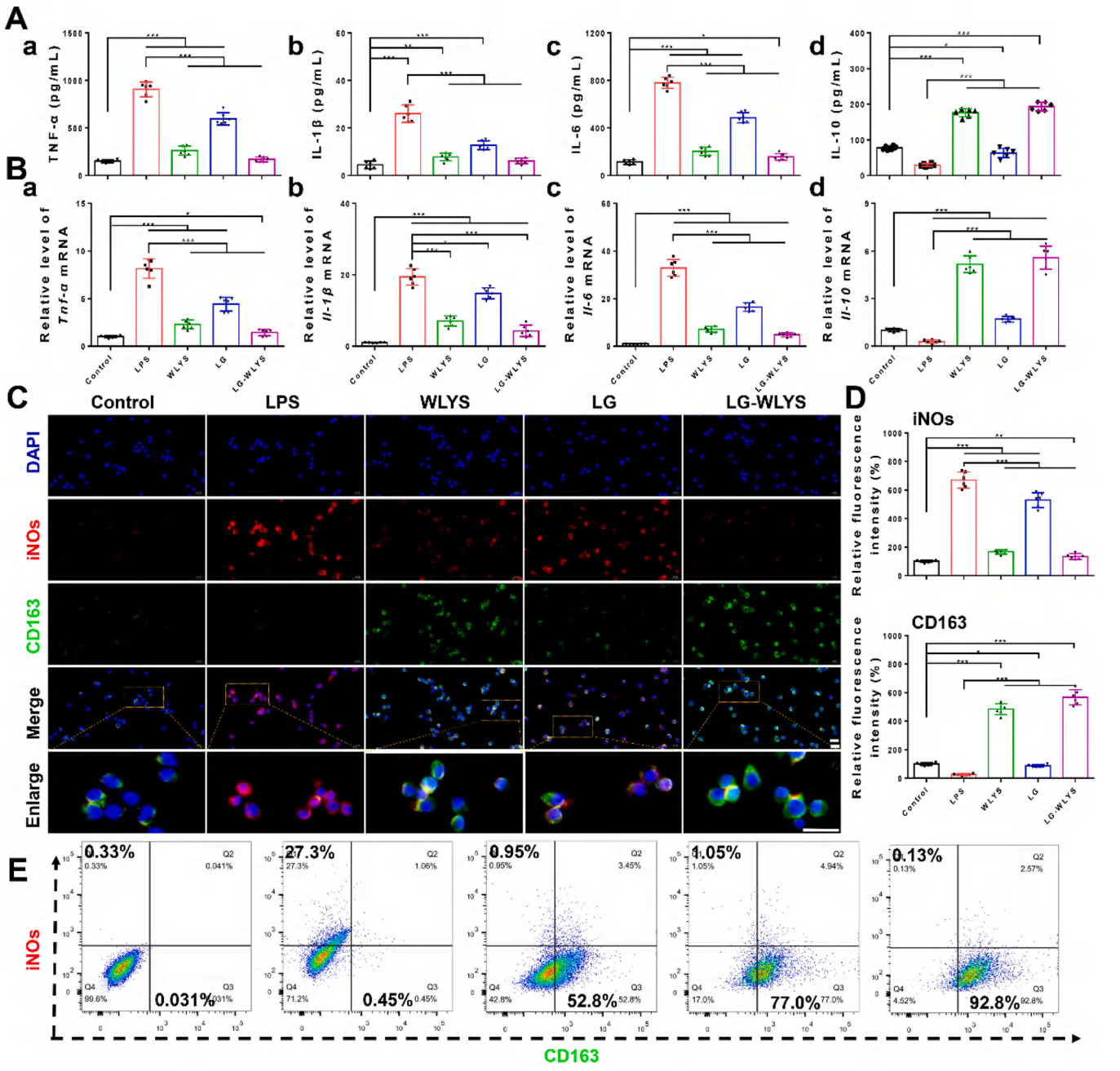

Fig. 3. Antioxidant capacity. (A) The cytokines level with RAW264.7 after incubation with different preparations for 24 h, including (a) TNF-α, (b) IL-1β, (c) IL-6, and (d) IL-10 (n = 6, mean ± SD). (B) The mRNA expression with RAW264.7 after incubation with the different preparations for 24 h, including (a) *Tnf-α,* (b) *Il-1β,* (c) *Il-6,* and (d) *Il-10* (n = 6, mean ± SD). (C) Macrophage polarization by iNOs (M1, red), CD163 (M2, green), and DAPI (blue). Scale bar = 200 μm. (D) Fluorescence quantification of Fig. 2 (C) (n = 6, mean ± SD). (E) Macrophage polarization by flow cytometry. * $P < 0.05$, * * $P < 0.01$, * ** $P < 0.001$.

(MDA) is a product of lipid peroxidation and an indicator of cellular oxidative damage. Activated macrophages release large amounts of NO, which disrupts the immune system and causes tissue damage. After treatment with LG-WLYS, the NO and MDA levels at the joint site were reduced ($P < 0.001$) (Fig. 7 A), alleviating inflammation. Glutathione (GSH) has antioxidant properties that help maintain normal immune function. Superoxide dismutase (SOD) plays a crucial role in maintaining the oxidative and antioxidant balance in the body [22]. After treatment with LG-WLYS, the GSH and SOD levels in the joints increased ($P < 0.001$) (Fig. 7 A), and the antioxidant capacity of the immune system was enhanced.

The spleen and thymus are the two major immune organs. The organ index reflects the strength of the immune function of the body. The rats in the model group showed an increase in organ index ($P < 0.05$) (Fig. 7 B), indicating a severe inflammatory response with splenomegaly in vivo. After treatment with LG-WLYS, organ indices were close to normal levels, suggesting that supplementation with LG-WLYS protected the viscera from over-enlargement of immune organs but did not reduce immunocompetence. The immunofluorescence results showed that LG-WLYS reduced ROS levels at the joint site (Fig. 7 C), inhibited chondrocyte apoptosis (Fig. 7 C), and promoted bone tissue repair.

The changes in the expression of inflammatory factors indicated that LG-WLYS effectively inhibited the inflammatory response. The number of M1 macrophages labeled with iNOs was increased in the RA group. Compared to normal rats, LG-WLYS changed this situation to a large degree and increased the number of M2 phenotype macrophages labeled

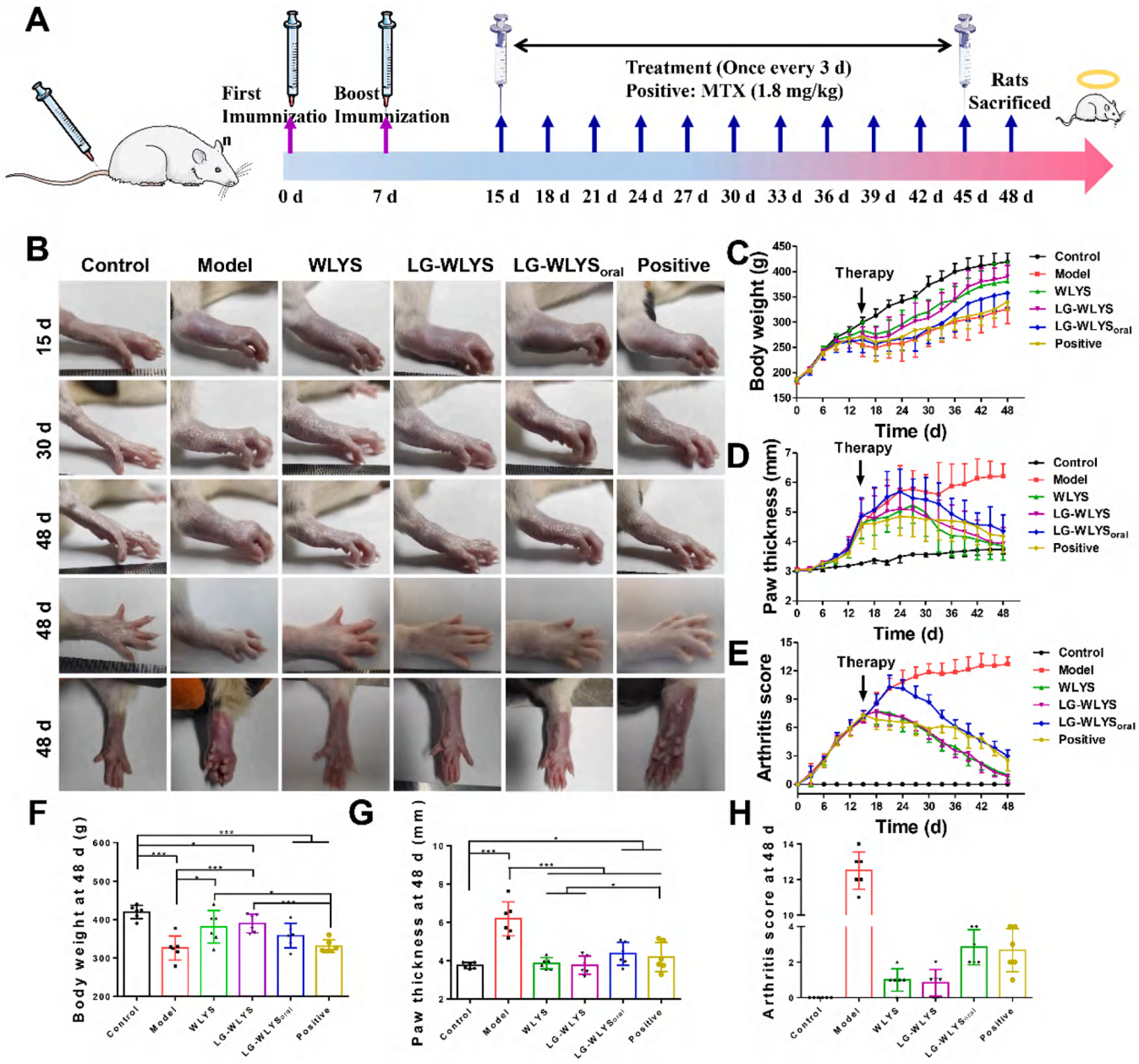

Fig. 4. In vivo therapeutic effects of LG-WLYS treatment in rats with RA. (A) Flowchart of the animal experiment. (B) Representative paw images of the different preparations-treated rats with RA after the different preparations treatment. (C) Body weight of rats on different treatment preparations (n = 6, mean ± SD). (D) Paw thickness changes in the RA model over time after different preparations (n = 6, mean ± SD). (E) Time-dependent arthritis score of the rats with RA determined at each evaluation time point (n = 6, mean ± SD). (F) Body weight of the rats with RA at 48 d (n = 6, mean ± SD). (G) Paw thickness of the rats with RA at 48 d (n = 6, mean ± SD). (H) Average arthritis score of the rats with RA (n = 6, mean ± SD). * $P < 0.05$, * ** $P < 0.001$.

with CD163 (Fig. 7 D). The decrease in pro-inflammatory macrophages and increase in anti-inflammatory cells in the joint proved that relief of joint inflammation could be achieved by regulating the proportion of inflammatory factors in the microenvironment using LG-WLYS.

3.7. Prophylactic experiments

LG-WLYS has outstanding effects in the treatment of RA. What excited us was that the effect of oral LG-WLYS was similar to that of the positive group (oral MTX). This prompted us to conduct an investigation. Rats were orally administered an appropriate concentration of LG-WLYS without restriction every day to investigate the incidence of rats with RA and to explore the interventional effect of LG-WLYS on inflammatory diseases and the impact on the immune system. The schedule of the prophylactic experiments is shown in Fig. 8 A. Rats received an unlimited daily oral dose of 200-fold diluted of LG-WLYS. After 20 days, the body weight gain was greater than that in the control group (Fig. 8 B). It is possible that the solution is rich in TEs, and that LG promotes the movement of cells in the gastrointestinal tract and increases digestive enzyme activity [23]. The next step was the RA modeling phase. To eliminate the effect of body weight, we selected healthy rats with body weights similar to those in the prophylaxis group as the control group (n = 6). Simultaneously, LG-WYLS was changed to a 10-fold dilution for unlimited daily consumption. There was a decrease in body weight in the model group, but a slow increase in body weight in the prophylaxis group (Fig. 8 C). On days 13–14 (33–34 days) after collagen injection, all rats in the model group developed RA symptoms, redness, swelling of the paws (Fig. 8 E), and difficulty in walking.

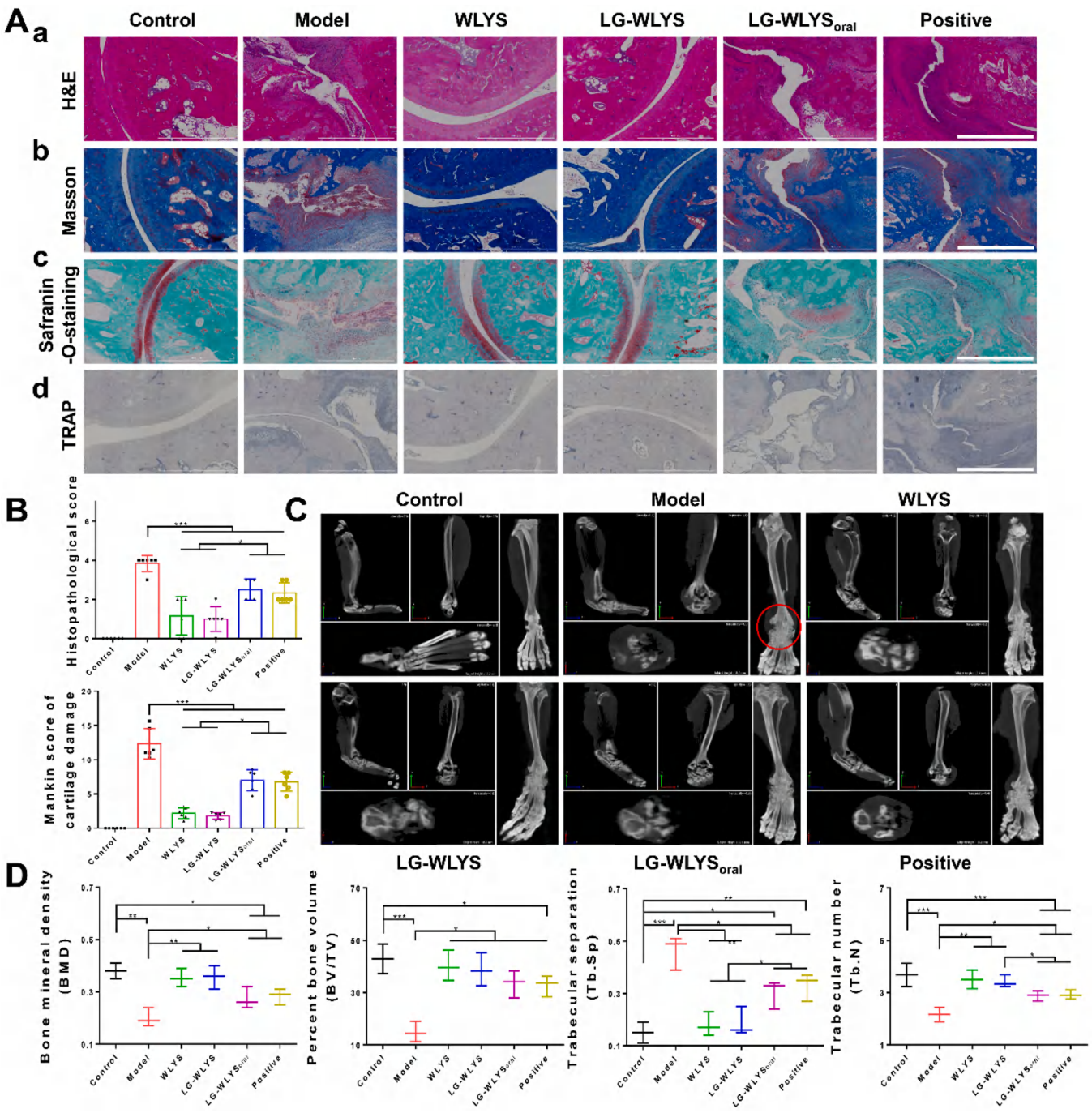

Fig. 5. Histopathological evaluation. (A) Histological assays with (a) H&E, (b) Masson, (c) Safranin-O-staining, and (d) TRAP staining of the joint tissue after the sample treatment. × 4, Scale bar = 1000 μm. (B) Histopathological and Mankin scores of different groups (n = 6, mean ± SD). (C) Representative paw X-ray images of the rats with RA with detailed ankle images for each group. The red indicates bone destruction and damage. (D) Quantitative results of bone status, including bone mineral density (BMD), bone volume-tissue volume (BV/TV), trabecular number (Tb. N), and trabecular separation (Tb. Sp) (n = 3, mean ± SD). * $P < 0.05$, * * $P < 0.01$, * ** $P < 0.001$.

In contrast, the prophylaxis group had a lower incidence and degree of morbidity. Eventually, only three rats in the prophylaxis group developed typical symptoms of RA at days 39, 42, and 45 (Fig. 8 D). At 51 days, we found that the prophylaxis group had red and swollen paws but could walk. The paws of the rats in the model group were severely deformed (Fig. 8 E). At this time, the rats in the prophylaxis group showed inflammatory cell infiltration in the joints. However, they did not developed lesions, had a large amount of mature bone tissue, and the cartilage was relatively intact with no osteoclasts observed (Fig. 8 F). In conclusion, drinking the correct concentration of LG-WLYS daily can prevent the development of inflammatory diseases, reduce treatment costs, and alleviate pain in patients.

3.8. Safety assessment

Evaluation of drug safety is an essential task in preclinical studies of new drugs. The safety of LG-WLYS was confirmed by blood biochemical analysis and H&E staining of the major organs in rats, where no organ damage was observed in the LG-WLYS group (Fig. 9 A and B). In comparison, we found some inflammatory cells in the liver and stomach

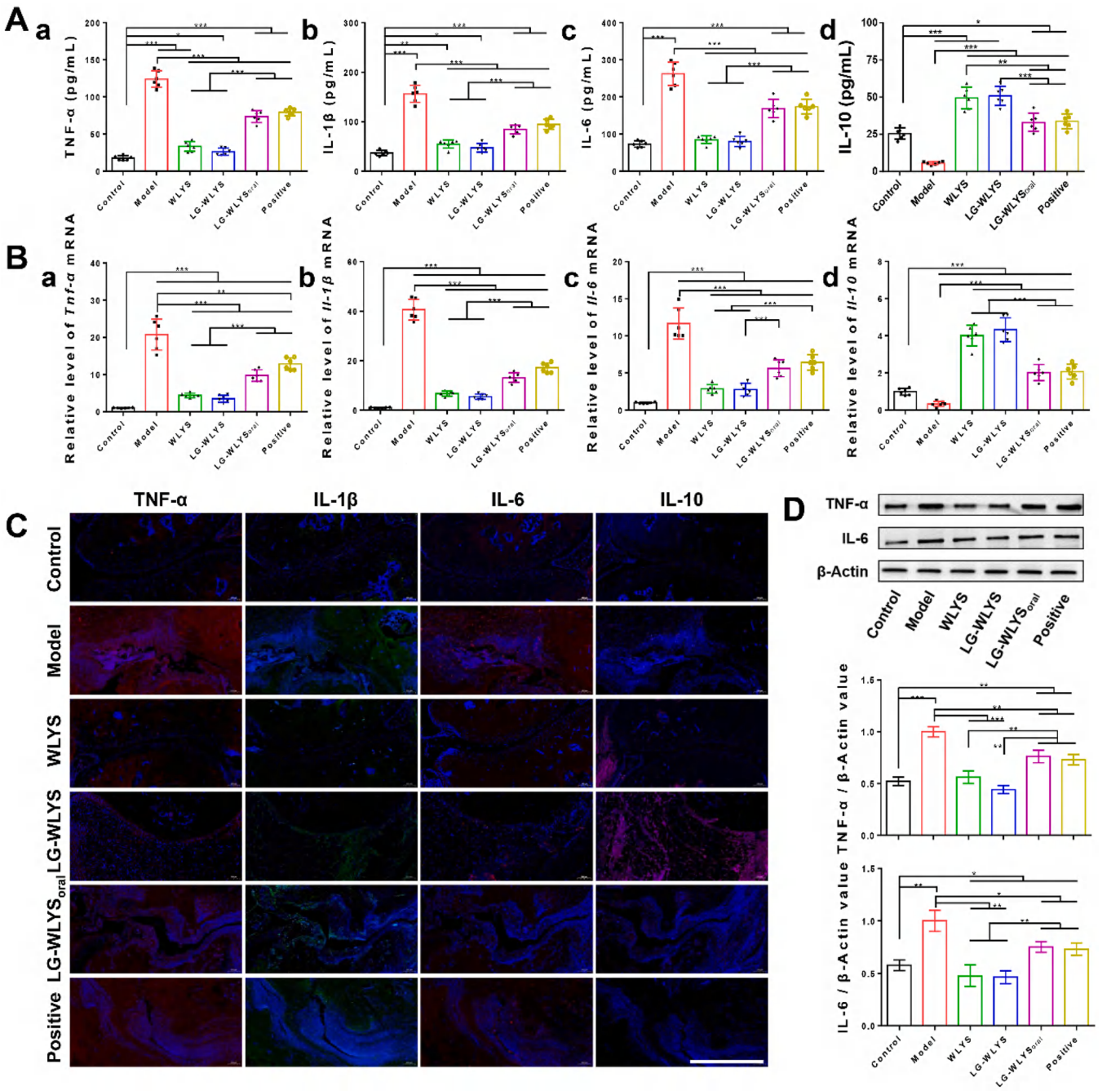

Fig. 6. Inflammation status. (A) The cytokines levels of (a) TNF-α, (b) IL-1β, (c) IL-6, and (d) IL-10 after treatment with the different preparations in RA rats (n = 6, mean ± SD). (B) Gene expression levels of (a) *Tnf-α,* (b) *Il-1β,* (c) *Il-6,* and (d) *Il-10* after treatment with the different preparations in rats with RA (n = 6, mean ± SD). (C) TNF-α, IL-1β, IL-6, and IL-10 immunofluorescence staining of joint sites. (D) The cytokine levels of TNF-α and IL-6 in different rats by western blot. * P < 0.05, * ** P < 0.001.

tissue sections of the positive group, which may be due to the side effects caused by long-term MTX administration[24,25].

4. Discussion

Although there is ongoing discussion on which TEs should be categorized as toxic, beneficial, or essential to living organisms, especially humans, approximately 20 known TEs are now defined as essential. TEs are crucial components of enzymes, proteins, and hormones and play critical roles in metabolism, cell growth and differentiation, and the immune system, affecting human physiology. Although the needs of healthy individuals are well-defined, disease needs remain poorly defined. The more severe the patient's condition, the greater the threat to nutritional and micronutrient status. In addition, the TEs status of many patients changes when they begin their ICU stay, and needs to be assessed at admission [26]. The accumulation of oxidative damage to biological components over time is a significant problem in immune senescence, and TEs interventions may help avoid or minimize this damage [27]. Taylor indicated that therapeutic uses provide unusual illustrations of the importance of TEs in human diseases [28].

The abnormal metabolism of serum TEs has also been reported in patients [12,29]. Some studies have found that TEs supplementation improves lipid peroxidation in the body, which is consistent with the results of the present study, suggesting that TEs can protect the body

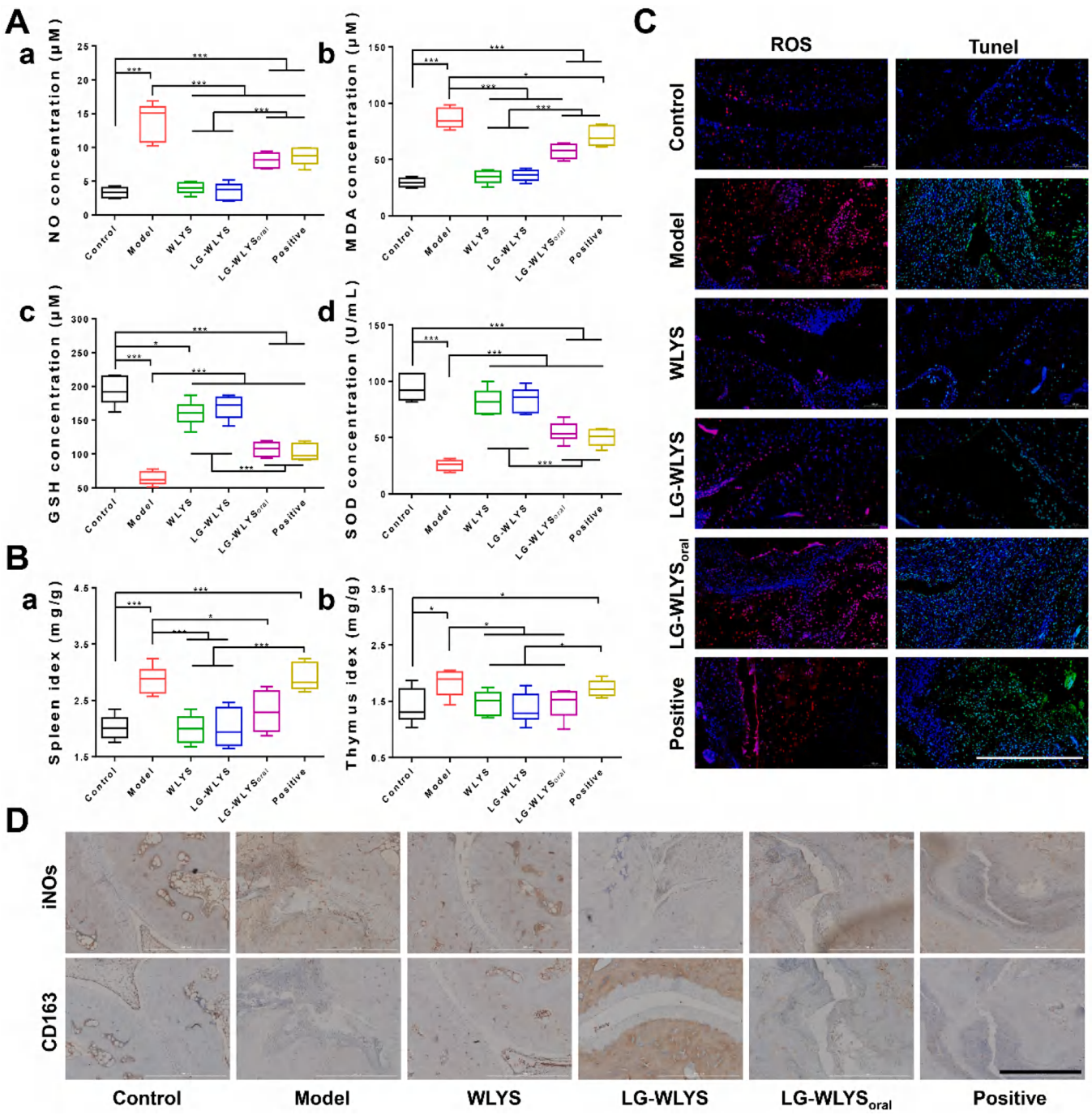

Fig. 7. (A) Concentration of oxidative stress indexes after treatment with the different preparations in rats with RA, including (a) NO, (b) MDA, (c) GSH, and (d) SOD (n = 6, mean ± SD). (B) Organ index of rats with RA after different treatments at 48 d, including (a) Spleen and (b) Thymus (n = 6, mean ± SD). (C) ROS and Tunel immunofluorescence staining of joint sites. (D) iNOs and CD163 immunocytochemistry of joint sites. Scale bar = 1000 μm. * P < 0.05, * * P < 0.01, * ** P < 0.001.

from oxidative damage by affecting the activity of antioxidant enzymes, which in turn reduces the increase in oxidation products [30]. The essential TEs, iron, zinc, selenium, and copper are critical for the immune and antioxidant defense systems [31]. Iron concentration was significantly lower in patients with RA [32]. Appropriate iron supplementation can improve the transporter levels in patients, increase the cellular uptake of MTX, and enhance its anti-inflammatory effect. This ensures a balanced uptake of iron and MTX to meet the growth and functional needs. Magnesium is the second most abundant intracellular cation in tissues [33] and a determining factor in the immune system [34]. Serum zinc levels are reduced in patients with RA because zinc proteins accumulate in inflamed tissues, leading to increased ceruloplasmin synthesis [35]. Manganese is a cofactor of many enzymes with metabolic and cellular energy-regulating functions. Manganese superoxide dismutase protects mitochondria from toxic oxidants [36]. Calcium is a cofactor for several enzymes. It is essential for intracellular functions as a messenger in cascading signaling reactions and for maintaining a stable blood pH [37]. As an antioxidant, selenium influences the activity of selenoproteins, such as glutathione peroxidase (GPx), which prevents membrane lipid peroxidation. When the GPx state is compromised, ROS and free radicals levels increase. A study presented low concentration of Se in the plasma of patients with RA as compared to control group [38]. Nickel deficiency causes growth inhibition and dermatitis. Molybdenum is considered an essential TEs

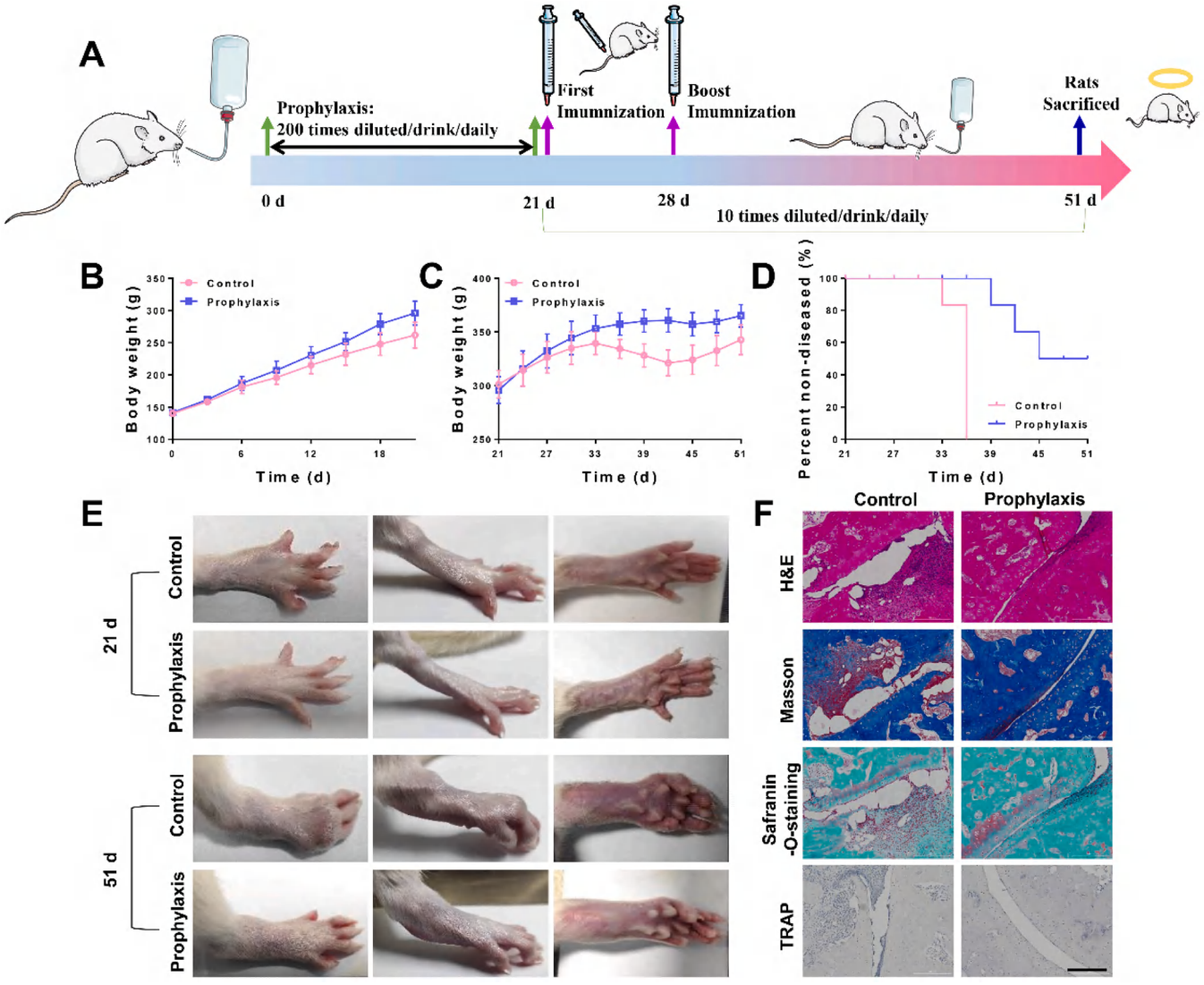

Fig. 8. Prophylactic study. (A) Schedule of prophylactic experiments. (B) Changes in body weight after drinking 200-fold diluted LG-WLYS without restriction (n = 6, mean ± SD). (C) Changes in body weight during the establishment of the RA model (n = 6, mean ± SD). (D) RA incidence in rats (n = 6). (E) Representative paw images of the prophylactic group rats at 21 and 51 days. (A) Histological assays with H&E, Masson, Safranin-O-staining, and TRAP staining of the joint tissue at 51 d. Scale bar = 200 μm.

because of its role in several enzymes, such as aldehyde oxidase, xanthine oxidase, and sulfite oxidase. Strontium is a TEs used in cell development and many physiological functions [39]. Strontium is a scavenger lipid peroxidation and prevents oxidative damage. Serum copper has been widely reported to play an essential role in humoral immunity against HCV infection, especially specific immunoglobulins such as IgA, IgM, and IgG[40]. Copper regulates immune responses via tyrosine hydroxylases.

Most commercially available TEs supplements are inorganic. Organic TEs are superior to inorganic TEs in terms of their absorption, utilization, and stability. The different forms and proportions of TEs are closely related to their efficacy. TEs can form coordination compounds that synergistically enhance the physiological activity of immune cells. Quality standards were set for the TEs solutions to ensure consistent batch quality. The solution contained dozens of TEs, and only 14 stypes of TEs with the highest concentrations selected as assay standards. The concentration ranges for the 14 TEs were specified, which helped eliminate batch-to-batch variation and ensured that patients received consistent efficacy and safety. The LG is an important source of nutrients for immune cells (such as lymphocytes and macrophages), providing energy and metabolism to support the normal function of the immune system. To improve the antioxidant effect of this solution while supplementing a variety of organic state TEs and LGs, regulating the homeostasis of the body's immune organs, promoting the maintenance of a balance between various TEs in the body, preventing the occurrence of inflammatory diseases, and maintaining the health of the human body.

Research suggests that multiple TEs may work together to produce a synergistic effect on cognitive function [41]. Niedermeier et al. explored the effect of chrysotherapy on TEs in patients with RA [42]. Our study evaluated the therapeutic efficacy of LG-WLYS for the treatment of RA. LG-WLYS reduced inflammatory cell infiltration, inhibited chondrocyte apoptosis, degraded collagen fibers in the joint cavity, improved joint damage, effectively alleviated paw swelling, lowered arthritis scores, and restored normal body weight in rats with RA. The therapeutic effect of LG-WLYS was superior to that of MTX alone. Moreover, LG-WLYS does not cause significant damage to organs in the body but rather strengthens the immune system. These results suggest that multiple TEs have cumulative and/or synergistic effects as antioxidants. Various studies have indicated that an elevated antioxidant defense system and decreased oxidative stress are key to RA treatment [43].

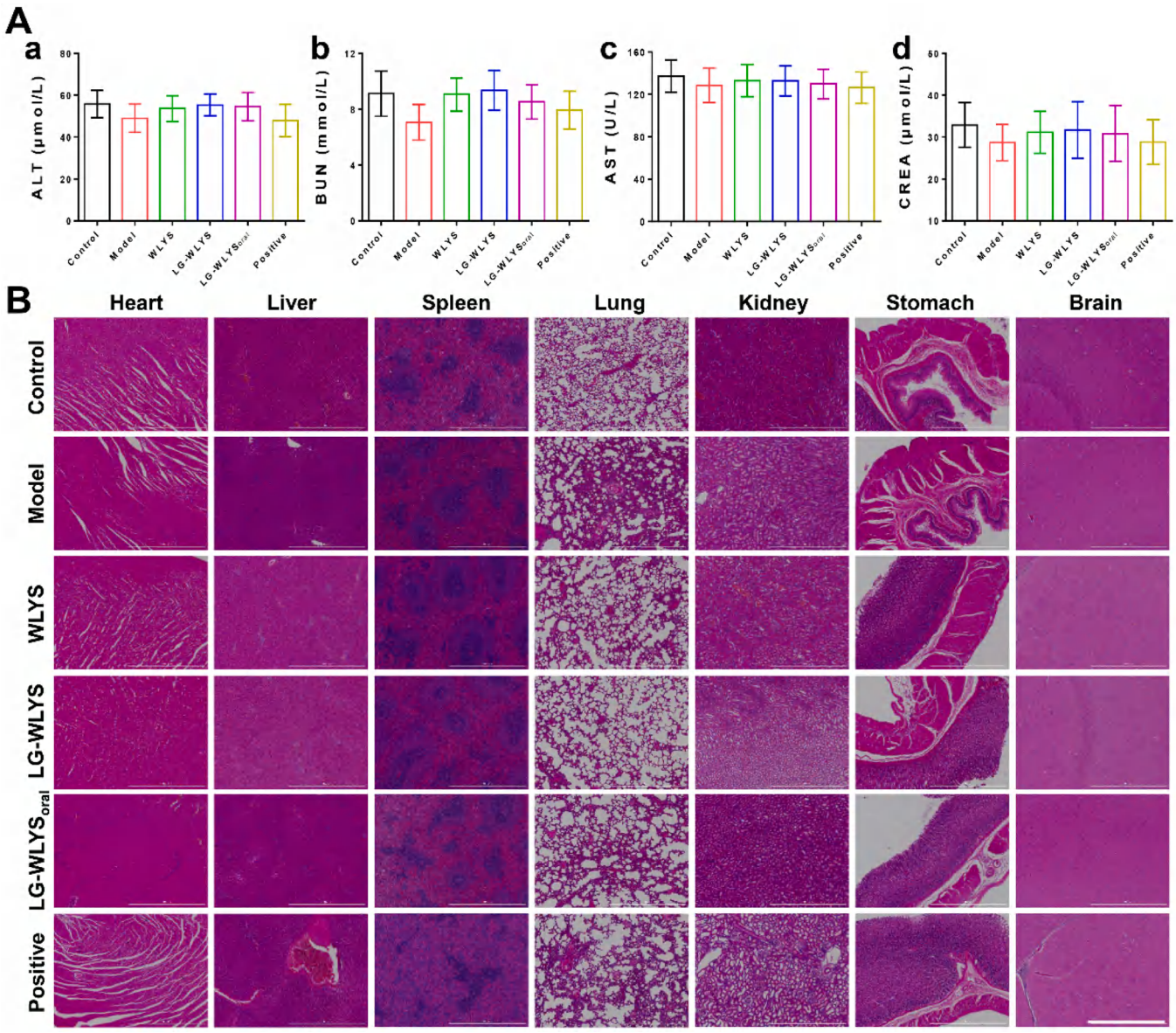

Fig. 9. Safety assessment. (A) Blood biochemistry of rats in rheumatoid arthritis experiment, including (a) ALT, (b) BUN, (c) AST, and (d) CREA (n = 6, mean ± SD). (B) H&E staining of RA rats. Scale bar = 1000 μm.

The pathogenesis of RA may be related to the interactions between genetic factors and their networks, T cell function, cytotoxic T lymphocyte-associated proteins, C-C motif chemokine receptors, and B cells [44]. At present, many signal transduction pathways of RA are known, including mitogen-activated protein kinase pathway, nuclear transcription factor pathway, phosphoinositide 3-kinase/protein kinase B pathway, and janus kinase/signal transduction and transcription activation protein pathway [45]. Disrupted immune homeostasis leads to the dysregulation of epigenetic factors, such as DNA methylation, histone modification, and micro-RNA, which activate autoantigens in RA. Rheumatoid factor and anti-citrullinated peptide antibodies are autoantibodies formed during RA. In addition, B cells contain antigens that lead to the production of cytokines and autoantibodies. Immune cells play an important role in RA via ROS signaling. ROS, like most physiological factors, are highly concentration dependent. ROS and inflammation go hand in hand in a cyclical relationship in which ROS are both signals and mediators of inflammation, and inflammation contributes to ROS production [46]. It is important to explore markers of inflammation and ROS [47]. Pro-inflammatory M1 macrophages constantly produce ROS, and high levels of ROS further induce the activation of M1-type macrophages. Excessive ROS production increases the levels of inflammatory cytokines, which accelerate the progression of RA. The results of this study showed that LG-WLYS induced macrophages to change from M1-type to M2-type, increased the content of antioxidant enzymes (GSH, SOD, and IL-10), decreased the levels of NO, MDA, TNF-α, IL-1β, and IL-6, scavenging ROS from the lesion site, decreasing the oxidative stress, inhibiting the apoptosis of chondrocytes, regulating inflammatory microenvironment, and decreasing inflammation response to exert the therapeutic effect for RA.

Our study highlights the potential of the LG-WLYS solution and provides a novel direction for the discovery and development of new drugs for the treatment of RA. The limitations of this study include the lack of elucidation of the changes in TEs status and potential alterations to the expression of plasma membrane transport systems in synovial structures in pathophysiological states. However, signaling pathways have not been well-studied. Although the interactions between toxic TEs in organisms and TEs that are essential for life are being increasingly considered, these interactions are complex. What is certain is that

impaired metabolism of TEs plays a role in the pathogenesis and progression of arthritis [10].

5. Conclusions

A solution of TEs containing various organic states was prepared using natural ores, with controlled concentration and standardized quality. In vivo experiments showed that the solution had favorable preventive and therapeutic effects on RA. This study demonstrates the potential of organic TEs to treat RA and inflammation caused by oxidative stress.

CRediT authorship contribution statement

Gao Zhonggao: Conceptualization, Data curation, Funding acquisition, Project administration, Resources, Supervision, Validation, Writing – review & editing. **Guo Jianpeng:** Funding acquisition. **Liu Yanhong:** Formal analysis, Writing – original draft. **Yin Jishan:** Formal analysis, Methodology. **Wang Shuangqing:** Data curation, Formal analysis, Investigation, Methodology, Visualization, Writing – original draft. **Wang Qiming:** Formal analysis. **Jin Mingji:** Funding acquisition, Resources.

Declaration of Competing Interest

Please declare any financial or personal interests that might be potentially viewed to influence the work presented. Interests could include consultancies, honoraria, patent ownership or other. If there are none state 'there are none'.

Acknowledgments

This work was supported by National Natural Science Foundation of China (82073778, 82104106), CAMS Innovation Fund for Medical Sciences (CIFMS) (2021-I2M-1–026, China), and Project of Jilin Province Science and Technology Development Plan (20200404086YY). No potential conflicts of interest were disclosed. All authors were involved in drafting the article or revising it critically for important intellectual content, and all authors approved the final version to be published.

Appendix A. Supporting information

Supplementary data associated with this article can be found in the online version at doi:10.1016/j.biopha.2023.116025.

References

[1] J. Liu, S. Song, R. Zhao, H.Y. Zhang, S.X. Zhang, The functions and networks of non-coding RNAs in the pathogenesis of rheumatoid arthritis, Biomed. Pharmacother. 163 (2023), 114707, https://doi.org/10.1016/j.biopha.2023.114707.

[2] X. Zhang, Y. Liu, C. Xiao, Y. Guan, Z. Gao, W. Huang, Research advances in nucleic acid delivery system for rheumatoid arthritis therapy, Pharmaceutics 15 (2023) 1237, https://doi.org/10.3390/pharmaceutics15041237.

[3] R. Ben Mrid, N. Bouchmaa, H. Ainani, R. El Fatimy, G. Malka, L. Mazini, Anti-rheumatoid drugs advancements: new insights into the molecular treatment of rheumatoid arthritis, Biomed. Pharmacother. 151 (2022), 113126, https://doi.org/10.1016/j.biopha.2022.113126.

[4] K.F. Zhai, H. Duan, C.Y. Cui, Y.Y. Cao, J.L. Si, H.J. Yang, Y.C. Wang, W.G. Cao, G. Z. Gao, Z.J. Wei, Liquiritin from glycyrrhiza uralensis attenuating rheumatoid arthritis via reducing inflammation, suppressing angiogenesis, and inhibiting MAPK signaling pathway, J. Agric. Food Chem. 67 (2019) 2856–2864, https://doi.org/10.1021/acs.jafc.9b00185.

[5] L. Zuo, E.R. Prather, M. Stetskiv, D.E. Garrison, J.R. Meade, T.I. Peace, T. Zhou, Inflammaging and oxidative stress in human diseases: from molecular mechanisms to novel treatments, Int. J. Mol. Sci. 20 (2019) 4472, https://doi.org/10.3390/ijms20184472.

[6] N. Nishimoto, J. Hashimoto, N. Miyasaka, K. Yamamoto, S. Kawai, T. Takeuchi, N. Murata, D. Der Van Heijde, T. Kishimoto, Study of active controlled monotherapy used for rheumatoid arthritis, an IL-6 inhibitor (SAMURAI): evidence of clinical and radiographic benefit from an x ray reader-blinded randomised controlled trial of tocilizumab, Ann. Rheum. Dis. 66 (2007) 1162–1167, https://doi.org/10.1136/ard.2006.068064.

[7] M. Jalili, S. Kolahi, S.R. Aref-Hosseini, M.E. Mamegani, A. Hekmatdoost, Beneficial role of antioxidants on clinical outcomes and erythrocyte antioxidant parameters in rheumatoid arthritis patients, Int. J. Prev. Med. 5 (2014) 835–840.

[8] R.M. Khadim, F.S. Al-Fartusie, Evaluation of some trace elements and antioxidants in sera of patients with rheumatoid arthritis: a case–control study, Clin. Rheumatol. 42 (2023) 55–65, https://doi.org/10.1007/s10067-022-06324-7.

[9] T. Frangos, W. Maret, Zinc and cadmium in the aetiology and pathogenesis of osteoarthritis and rheumatoid arthritis, Nutrients 13 (2021) 53, https://doi.org/10.3390/nu13010053.

[10] H.I. Afridi, T.G. Kazi, D. Brabazon, S. Naher, Association between essential trace and toxic elements in scalp hair samples of smokers rheumatoid arthritis subjects, 93–100, Sci. Total Environ. (2011) 412–413, https://doi.org/10.1016/j.scitotenv.2011.09.033.

[11] L. Chen, Q. Sun, S. Peng, T. Tan, G. Mei, H. Chen, Y. Zhao, P. Yao, Y. Tang, Associations of blood and urinary heavy metals with rheumatoid arthritis risk among adults in NHANES, 1999–2018, Chemosphere 289 (2022), 133147, https://doi.org/10.1016/j.chemosphere.2021.133147.

[12] Y. Ma, X. Zhang, D. Fan, Q. Xia, M. Wang, F. Pan, Common trace metals in rheumatoid arthritis: a systematic review and meta-analysis, J. Trace Elem. Med. Biol. 56 (2019) 81–89, https://doi.org/10.1016/j.jtemb.2019.07.007.

[13] J.R. Cerhan, K.G. Saag, L.A. Merlino, T.R. Mikuls, L.A. Criswell, Antioxidant micronutrients and risk of rheumatoid arthritis in a cohort of older women, Am. J. Epidemiol. 157 (2003) 345–354, https://doi.org/10.1093/aje/kwf205.

[14] D. Reyes-Hinojosa, C.A. Lozada-Pérez, Y. Zamudio Cuevas, A. López-Reyes, G. Martínez-Nava, J. Fernández-Torres, A. Olivos-Meza, C. Landa-Solis, M. C. Gutiérrez-Ruiz, E. Rojas del Castillo, K. Martínez-Flores, Toxicity of cadmium in musculoskeletal diseases, Environ. Toxicol. Pharmacol. 72 (2019), 103219, https://doi.org/10.1016/j.etap.2019.103219.

[15] P. Bonaventura, G. Courbon, A. Lamboux, F. Lavocat, H. Marotte, F. Albarède, P. Miossec, Protective effect of low dose intra-articular cadmium on inflammation and joint destruction in arthritis, Sci. Rep. 7 (2017), 2415, https://doi.org/10.1038/s41598-017-02611-5.

[16] N. Yu, F. Han, X. Lin, C. Tang, J. Ye, X. Cai, The association between serum selenium levels with rheumatoid arthritis, Biol. Trace Elem. Res. 172 (2016) 46–52, https://doi.org/10.1007/s12011-015-0558-2.

[17] D.C. McMillan, D. Maguire, D. Talwar, Relationship between nutritional status and the systemic inflammatory response: micronutrients, Proc. Nutr. Soc. 78 (2019) 56–57, https://doi.org/10.1017/s0029665118002501.

[18] A. Zuo, S. Wang, L. Liu, Y. Yao, J. Guo, Understanding the effect of anthocyanin extracted from Lonicera caerulea L. on alcoholic hepatosteatosis, Biomed. Pharmacother. 117 (2019), 109087, https://doi.org/10.1016/j.biopha.2019.109087.

[19] S. Wang, S. Meng, X. Zhou, Z. Gao, M.G. Piao, pH-responsive and mucoadhesive nanoparticles for enhanced oral insulin delivery: the effect of hyaluronic acid with different molecular weights, Pharmaceutics 15 (2023) 820, https://doi.org/10.3390/pharmaceutics15030820.

[20] K. Zhai, H. Duan, W. Wang, S. Zhao, G.J. Khan, M. Wang, Y. Zhang, K. Thakur, X. Fang, C. Wu, J. Xiao, Z. Wei, Ginsenoside Rg1 ameliorates blood–brain barrier disruption and traumatic brain injury via attenuating macrophages derived exosomes miR-21 release, Acta Pharm. Sin. B. 11 (2021) 3493–3507, https://doi.org/10.1016/j.apsb.2021.03.032.

[21] S. Wang, Y. Liu, Q. Sun, B. Zeng, C. Liu, L. Gong, H. Wu, L. Chen, M. Jin, J. Guo, Z. Gao, W. Huang, Triple cross-linked dynamic responsive hydrogel loaded with selenium nanoparticles for modulating the inflammatory microenvironment via PI3K/Akt/NF-κB and MAPK signaling pathways, Adv. Sci. 10 (2023), 2303167, https://doi.org/10.1002/advs.202303167.

[22] M. Liu, X. Sun, B. Chen, R. Dai, Z. Xi, H. Xu, Insights into manganese superoxide dismutase and human diseases, Int. J. Mol. Sci. 23 (2022) 15893, https://doi.org/10.3390/ijms232415893.

[23] S.M. Yoon, Micronutrient deficiencies in inflammatory bowel disease: trivial or crucial? Intest. Res. 14 (2016) 109–110, https://doi.org/10.5217/ir.2016.14.2.109.

[24] R. Katturajan, S. Evan Prince, L-carnitine and Zinc supplementation impedes intestinal damage in methotrexate-treated adjuvant-induced arthritis rats: reinstating enterocyte proliferation and trace elements, J. Trace Elem. Med. Biol. 78 (2023), 127188, https://doi.org/10.1016/j.jtemb.2023.127188.

[25] Y. Heo, M. Kim, G.G.D. Suminda, Y. Min, Y. Zhao, M. Ghosh, Y.O. Son, Inhibitory effects of Ganoderma lucidum spore oil on rheumatoid arthritis in a collagen-induced arthritis mouse model, Biomed. Pharmacother. 157 (2023), 114067, https://doi.org/10.1016/j.biopha.2022.114067.

[26] M.M. Berger, Nutrition and micronutrient therapy in critical illness should be individualized, J. Parenter. Enter. Nutr. 44 (2020) 1380–1387, https://doi.org/10.1002/jpen.2002.

[27] A. Raza, H. Johnson, A. Singh, A.K. Sharma, Impact of selenium nanoparticles in the regulation of inflammation, Arch. Biochem. Biophys. 732 (2022), 109466, https://doi.org/10.1016/j.abb.2022.109466.

[28] A. Taylor, Therapeutic uses of trace elements, Clin. Endocrinol. Metab. 14 (1985) 703–724, https://doi.org/10.1016/S0300-595X(85)80013-X.

[29] H.K. Al-Hakeim, S.R. Moustafa, K.M. Jasem, Serum cesium, rhenium, and rubidium in rheumatoid arthritis patients, Biol. Trace Elem. Res. 189 (2019) 379–386, https://doi.org/10.1007/s12011-018-1497-5.

[30] Y. Shi, Y. Zou, Z. Shen, Y. Xiong, W. Zhang, C. Liu, S. Chen, Trace elements, PPARs, and metabolic syndrome, Int. J. Mol. Sci. 21 (2020) 2612, https://doi.org/10.3390/ijms21072612.

[31] H. Wang, R. Zhang, J. Shen, Y. Jin, C. Chang, M. Hong, S. Guo, D. He, Circulating level of blood iron and copper associated with inflammation and disease activity of rheumatoid arthritis, Biol. Trace Elem. Res. 201 (2023) 90–97, https://doi.org/10.1007/s12011-022-03148-z.
[32] D.C. Das, I. Jahan, M.G. Uddin, M.M. Hossain, M.A.Z. Chowdhury, Z. Fardous, M. M. Rahman, A.K.M.H. Kabir, S.R. Deb, M.A.B. Siddique, A. Das, Serum CRP, MDA, vitamin C, and trace elements in bangladeshi patients with rheumatoid arthritis, Biol. Trace Elem. Res. 199 (2021) 76–84, https://doi.org/10.1007/s12011-020-02142-7.
[33] W.L. Baker, Treating arrhythmias with adjunctive magnesium: identifying future research directions, Eur. Hear. J. Cardiovasc. Pharmacother. 3 (2017) 108–117, https://doi.org/10.1093/ehjcvp/pvw028.
[34] G. Van Niekerk, M. Mitchell, A.M. Engelbrecht, Bone resorption: supporting immunometabolism, Biol. Lett. 14 (2018), 20170783, https://doi.org/10.1098/rsbl.2017.0783.
[35] S. Önal, M. Nazıroğlu, M. Çolak, V. Bulut, M.F. Flores-Arce, Effects of different medical treatments on serum copper, selenium and zinc levels in patients with rheumatoid arthritis, Biol. Trace Elem. Res. 142 (2011) 447–455, https://doi.org/10.1007/s12011-010-8826-7.
[36] P. Chen, J. Bornhorst, M. Aschner, Manganese metabolism in humans, Front. Biosci. - Landmark 23 (2018) 1655–1679, https://doi.org/10.2741/4665.
[37] M.A. Zoroddu, J. Aaseth, G. Crisponi, S. Medici, M. Peana, V.M. Nurchi, The essential metals for humans: a brief overview, J. Inorg. Biochem. 195 (2019) 120–129, https://doi.org/10.1016/j.jinorgbio.2019.03.013.
[38] P.H. Canter, B. Wider, E. Ernst, The antioxidant vitamins A, C, E and selenium in the treatment of arthritis: a systematic review of randomized clinical trials, Rheumatology 46 (2007) 1223–1233, https://doi.org/10.1093/rheumatology/kem116.
[39] H. Huang, J. Wang, J. Zhang, J. Cai, J. Pi, J. Xu, Inspirations of cobalt oxide nanoparticle based anticancer therapeutics, Pharmaceutics 13 (2021) 1599, https://doi.org/10.3390/pharmaceutics13101599.
[40] A.V. Ivanina, C. Hawkins, I.M. Sokolova, Interactive effects of copper exposure and environmental hypercapnia on immune functions of marine bivalves Crassostrea virginica and Mercenaria mercenaria, Fish. Shellfish Immunol. 49 (2016) 54–65, https://doi.org/10.1016/j.fsi.2015.12.011.
[41] B. jing Cheng, J. Wang, X. long Meng, L. Sun, B. Hu, H. biao Li, J. Sheng, G. mei Chen, F. biao Tao, Y. huan Sun, L. sheng Yang, The association between essential trace element mixture and cognitive function in Chinese community-dwelling older adults, Ecotoxicol. Environ. Saf. 231 (2022), 113182, https://doi.org/10.1016/j.ecoenv.2022.113182.
[42] W. Niedermeier, W.W. Prillaman, J.H. Griggs, The effect of chrysotherapy on trace metals in patients with rheumatoid arthritis, Arthritis Rheum. 14 (1971) 533–538, https://doi.org/10.1002/art.1780140413.
[43] N. Qamar, P. John, A. Bhatti, Emerging role of selenium in treatment of rheumatoid arthritis: an insight on its antioxidant properties, J. Trace Elem. Med. Biol. 66 (2021), 126737, https://doi.org/10.1016/j.jtemb.2021.126737.
[44] K.F. Zhai, H. Duan, Y. Chen, G.J. Khan, W.G. Cao, G.Z. Gao, L.L. Shan, Z.J. Wei, Apoptosis effects of imperatorin on synoviocytes in rheumatoid arthritis through mitochondrial/caspase-mediated pathways, Food Funct. 9 (2018) 2070–2079, https://doi.org/10.1039/c7fo01748k.
[45] S. Liu, H. Ma, H. Zhang, C. Deng, P. Xin, Recent advances on signaling pathways and their inhibitors in rheumatoid arthritis, Clin. Immunol. 230 (2021), 108793, https://doi.org/10.1016/j.clim.2021.108793.
[46] M. Mittal, M.R. Siddiqui, K. Tran, S.P. Reddy, A.B. Malik, Reactive oxygen species in inflammation and tissue injury, Antioxid. Redox Signal. 20 (2014) 1126–1167, https://doi.org/10.1089/ars.2012.5149.
[47] S.X. Ren, B. Zhang, Y. Lin, D.S. Ma, H. Yan, Selenium nanoparticles dispersed in phytochemical exert anti-inflammatory activity by modulating catalase, GPx1, and COX-2 gene expression in a rheumatoid arthritis rat model, Med. Sci. Monit. 25 (2019) 991–1000, https://doi.org/10.12659/MSM.912545.